Hindawi
Advances in Civil Engineering
Volume 2020, Article ID 9170706, 11 pages
https://doi.org/10.1155/2020/9170706

Research Article

New Maxwell Creep Model Based on Fractional and Elastic-Plastic Elements

Hao Tang[1,2] **Dongpo Wang**[3] **and Zhao Duan**[2]

[1]*Geological Research Institute for Coal Green Mining, Xi'an University of Science and Technology, Xi'an 710054, China*
[2]*College of Geology and Environment, Xi'an University of Science and Technology, Xi'an 710054, China*
[3]*State Key Laboratory of Geohazard Prevention and Geoenvironment Protection, Chengdu University of Technology, Chengdu 610059, China*

Correspondence should be addressed to Dongpo Wang; wangdongpo@imde.ac.cn

Received 29 November 2019; Accepted 17 January 2020; Published 10 February 2020

Academic Editor: Salvatore Grasso

Creep models are mainly used to describe the rheological behaviour of geotechnical materials. An important research focus for studying creep in geotechnical materials is the development of a model with few parameters and good simulation performance. Hence, in this study, by replacing the Newtonian dashpot and spring in the classical Maxwell model with fractional and elastic-plastic elements, a new Maxwell creep model based on fractional derivatives and continuum damage mechanics was developed. One- and three-dimensional (1D/3D) creep equations of the new Maxwell creep model were derived. The 1D creep equation of the new model was used to fit existing creep data of rock salt, and the 3D creep equation was used to fit the creep data of remolded loess. The model curves matched the creep data very well, showing considerably higher accuracy than other models. Furthermore, a sensitivity study was carried out, showing the effects of the fractional derivative order β and exponent α on the creep strain of rock salt. This new model is simple with few parameters and can effectively simulate the complete creep behaviour of geotechnical materials.

1. Introduction

Creep models are abstract methods for expressing the creep characteristics of geotechnical materials. The creep behaviour of geotechnical materials can be described using differential, integral, or empirical creep equations, and their creep characteristics can be represented using a theoretical creep curve approximating the real creep curve. As a differential creep model, the component model has been applied and expanded by many researchers because of its simple structure and clear physical meaning (e.g., Maxwell, Kelvin, Burgers, and Nishihara models). It is well known that the deformation of geotechnical materials during creep tests can be divided into four stages: instantaneous deformation, transient creep, steady creep, and accelerated creep. These different deformation stages have their own characteristics, and it is difficult to build a model that can simulate all four deformation stages. Therefore, many scholars are looking for new methods to improve the component model for representing all the deformation stages.

Fractional calculus involves derivative and integration operators that are applied to fractional orders. As one of the generalisations of classical calculus, fractional calculus is used widely in various fields of science and engineering. Because of the long history dependence, or the so-called memory effect, fractional operators are powerful tools for modelling the viscoelastic behaviour of materials, particularly for building a time-dependent constitutive model. Because of the pioneering work of Scott-Blair [1], who proposed a fractional element analogous to the classical Newtonian dashpot, many creep models based on fractional calculus have been developed in recent years. Rogers [2], Bagly and Torvik [3, 4], and Koeller [5] have performed remarkable studies on creep models using fractional calculus. Welch et al. [6] proposed a four-parameter creep model to characterise the viscoelastic creep of polymeric

materials using fractional calculus. Zhou et al. [7, 8] proposed a fractional derivative model to describe the creep behaviour of rock salt. Yin et al. [9] established a variable-order fractional creep model to describe the evolution of the mechanical properties of soft soils. Kang et al. [10] applied fractional calculus to build a nonlinear creep model for coal. Celauro et al. [11] proposed a fractional derivative model to describe the viscoelastic behaviour of asphalt mixtures. In addition, some scholars [12–17] have developed relevant creep models using fractional calculus. Although fractional calculus is widely adopted in developing creep models, a key limitation is its inability to describe the accelerated creep phase of geotechnical materials; in terms of the mathematical description of the obtained curves, fractional calculus cannot suitably describe the accelerated creep stage of rocks.

Therefore, using a continuum damage mechanics approach, some creep models incorporate a damage factor to describe the accelerated creep phase. Moreover, the method of introducing a damage factor provides a clear physical meaning in characterising creep damage. Mazotti and Savoia [18] proposed a creep damage model for concrete, considering the combined effect of nonlinear viscous strain evolution and crack nucleation and propagation at high stress levels. Verstrynge et al. [19] proposed an improved Burges model by introducing a viscous damage parameter, which reflected the accumulation of damage over a long period in a masonry structure. Ma et al. [20] proposed a three-dimensional (3D) creep damage model combined with the generalised Hoek–Brown model and validated the same with a series of strength and creep tests for bedded rock salt. Cao et al. [21] proposed an elastic-plastic damage cell model by introducing the damage theory and law of damage proposed by Kachanov [22], which can describe the nonlinear or accelerated rock creep process. In addition, many scholars [23–26] have developed creep models for rock by applying continuum damage mechanics. However, despite recent improvements in the creep models for geotechnical materials, there is no simple or universal model that can fully describe their viscoelastic-plastic creep behaviour. Models with simple structures cannot effectively simulate the complete creep behaviour of geotechnical materials; moreover, many of the effective models have more parameters. Therefore, developing a model with few parameters and better simulation performance is the key goal in the study of creep constitutive models.

The Maxwell model is the simplest creep model with only two elements and two parameters. However, its mathematical equation can only express linear material creep. Therefore, the original Maxwell model requires improvements. In recent years, some scholars [27–32] have applied fractional calculus to improve the original Maxwell model. These improved Maxwell models can approximately describe the partial nonlinear creep deformation of geotechnical materials. However, these improved Maxwell models are unable to describe the accelerated creep phase effectively.

Therefore, in this paper, we present a new Maxwell creep model based on fractional and elastic-plastic elements to characterise the creep behaviour of rock salt and remolded loess under different stress states. The advantages of the model were identified through validation and sensitivity analysis.

2. New Maxwell Creep Model

2.1. Fractional Element. From a mathematical perspective, the constitutive equations of spring and dashpot elements can be described as follows:

$$\begin{cases} \sigma(t) = E\dfrac{\mathrm{d}^0\varepsilon(t)}{\mathrm{d}t^0}, \\ \\ \sigma(t) = \eta\dfrac{\mathrm{d}^1\varepsilon(t)}{\mathrm{d}t^1}. \end{cases} \tag{1}$$

As shown in equation (1), the stress of an elastic solid is proportional to the zeroth-order derivative of the strain, whereas the stress of a Newtonian fluid is proportional to the first-order derivative of the strain. Based on the mathematical transformation relations mentioned above, a general constitutive equation for a viscoelastic body may be written as

$$\sigma(t) = \xi\frac{\mathrm{d}^\beta\varepsilon(t)}{\mathrm{d}t^\beta}, \quad 0 \le \beta \le 1. \tag{2}$$

Equation (2) is known as the Scott-Blair [1] fractional element, and it is commonly referred to as the Abel dashpot. The symbolic representation of this element is shown in Figure 1. In equation (2), $\sigma(t)$ and $\varepsilon(t)$ are the stress and strain, respectively; ξ is the viscosity coefficient of the material, with units of (stress·time)$^\beta$; t is the time; β is the fractional order, with $0 \le \beta \le 0$. Equation (2) degrades to show the constitutive relationship of a spring when $\beta = 0$ and that of a dashpot when $\beta = 1$. However, when $0 < \beta < 1$, the fractional element can exhibit the characteristics of both a spring and dashpot.

Fractional calculus can be defined in many ways, such as Riemann–Liouville and Caputo derivatives [33]. The Riemann–Liouville fractional integration of function $f(t)$ with order β is defined as

$${}_0D_t^{-\beta}f(t) = \frac{\mathrm{d}^{-\beta}f(t)}{\mathrm{d}t^{-\beta}} = \int_{t_0}^{t}\frac{(t-\tau)^{\beta-1}}{\Gamma(\beta)}f(\tau)\mathrm{d}\tau, \tag{3}$$

and the fractional derivative of function $f(t)$ with order β is defined as

$${}_0D_t^{\beta}f(t) = \frac{\mathrm{d}^{\beta}f(t)}{\mathrm{d}t^{\beta}} = \frac{\mathrm{d}^n}{\mathrm{d}t^n}\left[{}_{t_0}D_t^{-(n-\beta)}f(t)\right], \tag{4}$$

where $\beta > 0$ and $n-1 < \beta \le n$ (n is a positive integer), and $\Gamma(x)$ is the gamma function defined as

$$\Gamma(x) = \int_0^\infty e^{-t}t^{x-1}\mathrm{d}t, \quad (\mathrm{Re}(x) > 0). \tag{5}$$

If equation (2) is considered in terms of its physical interpretation, it can be used to characterise the mechanical properties of geotechnical materials ranging between an ideal solid and ideal fluid during creep. Thus, if the stress $\sigma(t)$ is a constant, the fractional element will describe the change

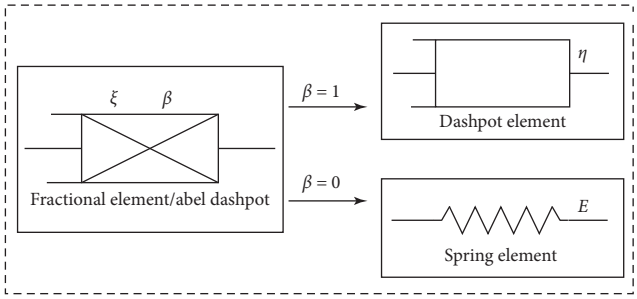

Figure 1: Fractional element.

in the creep behaviour of the geotechnical materials. The creep equation of materials can be obtained by employing the Riemann–Liouville fractional calculus theory as follows:

$$\varepsilon(t) = \frac{\sigma_0}{\xi} \cdot \frac{t^{\beta}}{\Gamma(1+\beta)}, \quad 0 < \beta < 1, \tag{6}$$

where σ_0 denotes the constant stress level. Two parameters are included in equation (6), namely, the viscosity coefficient ξ and fractional order β. ξ Reflects viscosity of the materials, and β reflects the variation laws of the creep curves of materials. Substituting $\sigma(t) = 10$ MPa and $\xi = 2000$ MPa·h$^{\beta}$ into equation (6), a series of creep curves with different β values were obtained, as shown in Figure 2.

As observed in Figure 2, when the stress remains constant, the creep strain increases gradually as β increases. When $0 < \beta < 1$, the morphological characteristics of the creep curves demonstrate that the fractional element can be used to describe the transient and steady creep phase of rock.

2.2. Elastic-Plastic Element. The deformation of geotechnical materials during a creep test can be divided into four phases: instantaneous deformation, transient creep, steady creep, and accelerated creep. Based on previous research experience, many classical component models can simulate the first three deformation stages reliably. However, many of the proposed models have limitations in terms of simulating the accelerated creep stage. Therefore, it is always challenging to simulate the accelerated creep stage; many researchers have tried to address this problem by proposing various nonlinear elements. Through comparison and analysis, a type of elastic-plastic element based on the damage rate change proposed by Cao et al. [21] was identified for succinct and accurate simulation of the accelerated creep stage in this study. Based on the damage variable proposed by Kachanov [22], considering the critical stress (σ_s) of the geotechnical material during creep, the new damage variable improved by Cao et al. [21] can be written as

$$D = \begin{cases} 0, & \sigma < \sigma_S, \\ 1 - \left(1 - \frac{t}{t_F}\right)^{\alpha}, & \sigma \geq \sigma_S, \end{cases} \tag{7}$$

where t_F is the time from initial deformation to final failure and α is the material constant. Substituting equation (7) into the creep constitutive relation of the elastic element, the

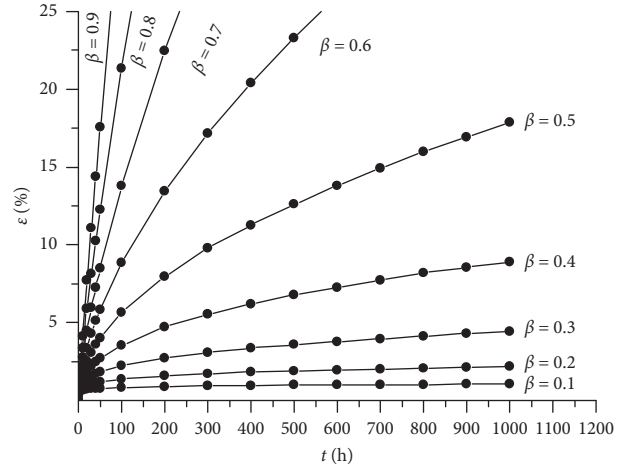

Figure 2: Fractional element creep curves for a range of fractional orders.

creep equation of the elastic-plastic element can be expressed as

$$\varepsilon = \begin{cases} \frac{\sigma}{E}, & \sigma < \sigma_S, \\ \frac{\sigma}{E}\left(1 - \frac{t}{t_F}\right)^{-\alpha}, & \sigma \geq \sigma_S. \end{cases} \tag{8}$$

The constitutive equation of the elastic-plastic element is effective to a certain extent for simulating the creep characteristics of geotechnical materials. When $\sigma < \sigma_s$, the elastic-plastic element degenerates into a spring element, and when $\sigma \geq \sigma_s$ and the time is t_F, the element can describe the accelerated creep phases of geotechnical materials.

2.3. New Maxwell Creep Model. As mentioned previously, the deformation rock during a creep test can be divided into four phases: instantaneous deformation, transient creep, steady creep, and accelerated creep. Therefore, an excellent creep model must have the ability to simulate the intact creep behaviour of rock, especially in the accelerated creep phase. To achieve this objective, a new creep model based on a fractional element and an elastic-plastic element placed in series was developed, as shown in Figure 3. This model is referred to as the new Maxwell creep model.

Based on the connection characteristics of the elements, in the one-dimensional (1D) creep state, this new Maxwell creep model satisfies the following relationship:

$$\begin{cases} \varepsilon = \frac{\sigma}{E} + \frac{\sigma}{\xi} \cdot \frac{t^{\beta}}{\Gamma(1+\beta)}, & \sigma < \sigma_s,\ 0 < \beta < 1, \\ \varepsilon = \frac{\sigma}{E\left(1 - \left(t/t_F\right)\right)^{\alpha}} + \frac{\sigma}{\xi} \cdot \frac{t^{\beta}}{\Gamma(1+\beta)}, & \sigma \geq \sigma_s,\ 0 < \beta < 1, \end{cases} \tag{9}$$

where E and ξ are the elastic modulus and viscosity coefficient of loess, respectively; α is a constant pertaining to the properties of the rock; and β is the fractional order.

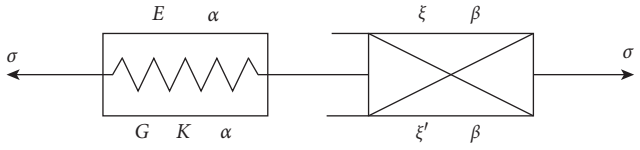

Figure 3: New Maxwell creep model.

Equation (9) shows that the new Maxwell creep model will degenerate into spring and fractional elements in series when the loading stress is lower than the critical stress. Thus, the new model can be used to describe instantaneous deformation, transient creep, and steady creep of rock. When the loading stress is larger than the critical stress, this model can be used to describe the entire deformation process, including accelerated creep. This model has the advantage of using only four parameters, thus resulting in a simple structure.

In the 3D stress state, the stress tensor σ_{ij} can be decomposed into the stress sphere tensor σ_m and partial tensor S_{ij}. Similarly, the strain tensor ε_{ij} can be decomposed into the strain sphere tensor ε_m and partial tensor e_{ij}. Their relationship can be expressed as follows:

$$\begin{cases} \sigma_{ij} = S_{ij} + \delta_{ij}\sigma_m, \\ \varepsilon_{ij} = e_{ij} + \delta_{ij}\varepsilon_m, \end{cases} \tag{10}$$

where δ_{ij} is the Kronecker symbol. According to the generalised Hook's law, the 3D constitutive equation for a Hookean body can be written as

$$\varepsilon_{ij}^{e} = \frac{S_{ij}}{2G} + \frac{\sigma_m}{3K}\delta_{ij}, \tag{11}$$

where ε_{ij}^{e}, G, and K represent the strain tensor, shear modulus, and volume modulus of the Hookean body, respectively. Assuming that the material rheology is mainly governed by shear deformation, the 3D constitutive relationship of a viscoelastic body (fractional element) can be expressed as

$$e_{ij}^{ve} = \frac{S_{ij}}{2\xi'} \cdot \frac{t^{\beta}}{\Gamma(1+\beta)}, \tag{12}$$

where e_{ij}^{ve} and ξ' are the partial strain tensor and shear modulus of the viscoelastic body, respectively.

Based on equations (11) and (12), the 3D creep equation of the new Maxwell creep model can be written as

$$\begin{cases} \varepsilon_{ij} = \dfrac{S_{ij}}{2G} + \dfrac{\sigma_m}{3K}\delta_{ij} + \dfrac{S_{ij}}{2\xi'} \cdot \dfrac{t^{\beta}}{\Gamma(1+\beta)}, & S_{ij} < \sigma_s,\ 0 < \beta < 1, \\ \varepsilon_{ij} = \dfrac{S_{ij}}{2G^*} + \dfrac{\sigma_m}{3K}\delta_{ij} + \dfrac{S_{ij}}{2\xi'} \cdot \dfrac{t^{\beta}}{\Gamma(1+\beta)}, & S_{ij} \geq \sigma_s,\ 0 < \beta < 1, \end{cases} \tag{13}$$

where $G^* = G(1 - D)$.

When the triaxial compression creep stress state is $\sigma_2 = \sigma_3$ and constant, with all levels of load σ_1 being constant, then

$$\begin{cases} \sigma_m = \dfrac{1}{3}(\sigma_1 + 2\sigma_3), \\ S_{11} = \sigma_1 - \sigma_m = \dfrac{2}{3}(\sigma_1 - \sigma_3). \end{cases} \tag{14}$$

and thus equation (13) can be rewritten as

$$\begin{cases} \varepsilon_{ij} = \dfrac{\sigma_1 - \sigma_3}{3G} + \dfrac{\sigma_1 + 2\sigma_3}{9K} + \dfrac{\sigma_1 - \sigma_3}{3\xi'} \cdot \dfrac{t^{\beta}}{\Gamma(1+\beta)}, \\ \qquad\qquad \sigma_1 - \sigma_3 < \sigma_s,\ 0 < \beta < 1, \\ \varepsilon_{ij} = \dfrac{\sigma_1 - \sigma_3}{3G\left(1 - \left(t/t_F\right)\right)^{\alpha}} + \dfrac{\sigma_1 + 2\sigma_3}{9K} + \dfrac{\sigma_1 - \sigma_3}{3\xi'} \cdot \dfrac{t^{\beta}}{\Gamma(1+\beta)}, \\ \qquad\qquad \sigma_1 - \sigma_3 \geq \sigma_s,\ 0 < \beta < 1. \end{cases} \tag{15}$$

3. Analysis of New Maxwell Creep Model in 1D Creep State

3.1. Data Preparation. Based on previous research results [34], typical axial creep experimental data for rock salt in the Changshan Salt Mine (Zigong City, Sichuan Province, China) were used to verify the proposed new Maxwell creep model. Figure 4 shows the axial creep curves for rock salt under loading stresses of 9.93, 14.41, and 14.72 MPa. The creep curve for a loading stress of 14.41 MPa exhibits the three typical creep phases and thus represents the typical intact creep behaviour of rock. The creep curve for a loading stress of 9.93 MPa is characteristic of the case when the loading stress is lower than the yield stress and that for a loading stress of 14.72 MPa is characteristic of the case when the loading stress is larger than the yield stress.

3.2. Parameter Determination. We used the 1D creep equation of the new Maxwell model to fit the experimental data for rock salt shown above. The parameters in Equation (9) can be determined using the Levenberg–Marquardt method, which is a nonlinear least-squares fitting method, and the results are presented in Table 1. The efficacy of the proposed creep model in fitting the rock salt data is shown in Figure 5. To further analyse the simulation capability of the proposed creep model, we compared it to the Burgers and Nishihara models, as shown in Figure 5; the parameters of the Burgers and Nishihara models are also given in Table 1.

From the analysis results presented in Table 1, it is seen that the coefficient of determination $R^2 > 0.9$, indicating that the new Maxwell creep model proposed herein is in good agreement with the experimental data of rock salt. Moreover, Figure 5 shows that the new Maxwell creep model has good consistency with the experimental data, which further proves that the proposed model is effective and reliable. In addition, Figure 5 shows that the new Maxwell creep model provides better simulation of the creep properties of rock salt

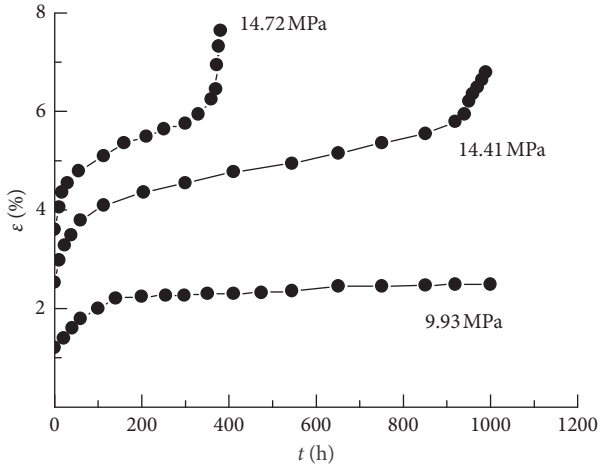

Figure 4: Axial creep curves for Changshan rock salt.

Table 1: Parameters determined through fitting analysis based on creep tests of rock salt.

New Maxwell creep model	σ (MPa)	E (GPa)	ξ (GPa·h$^{\beta}$)	β	α	σ_s (MPa)	t_F (h)	R^2
	9.93	0.875	4.544	0.260		13.5		0.918
	14.41	0.590	3.662	0.252	0.191	13.5	1056	0.988
	14.72	0.415	3.904	0.241	0.110	13.5	385	0.978
Burgers model	σ (MPa)	E_H (GPa)	E_K (GPa)	η_K (GPa·h)	η (GPa·h)	R^2		
	9.93	0.860	0.931	3446.914	63.999	0.993		
	14.41	0.568	1.271	541.794	30.426	0.968		
	14.72	0.410	2.222	18.242	221.010	0.901		
Nishihara model	σ (MPa)	E_H (GPa)	E_K (GPa)	η_K (GPa·h)	η_S (GPa·h)	σ_s (MPa)	R^2	
	9.93	0.829	0.820	79.527		13.5	0.975	
	14.41	0.568	1.271	30.425	34.214	13.5	0.968	
	14.72	0.410	2.222	18.242	18.317	13.5	0.901	

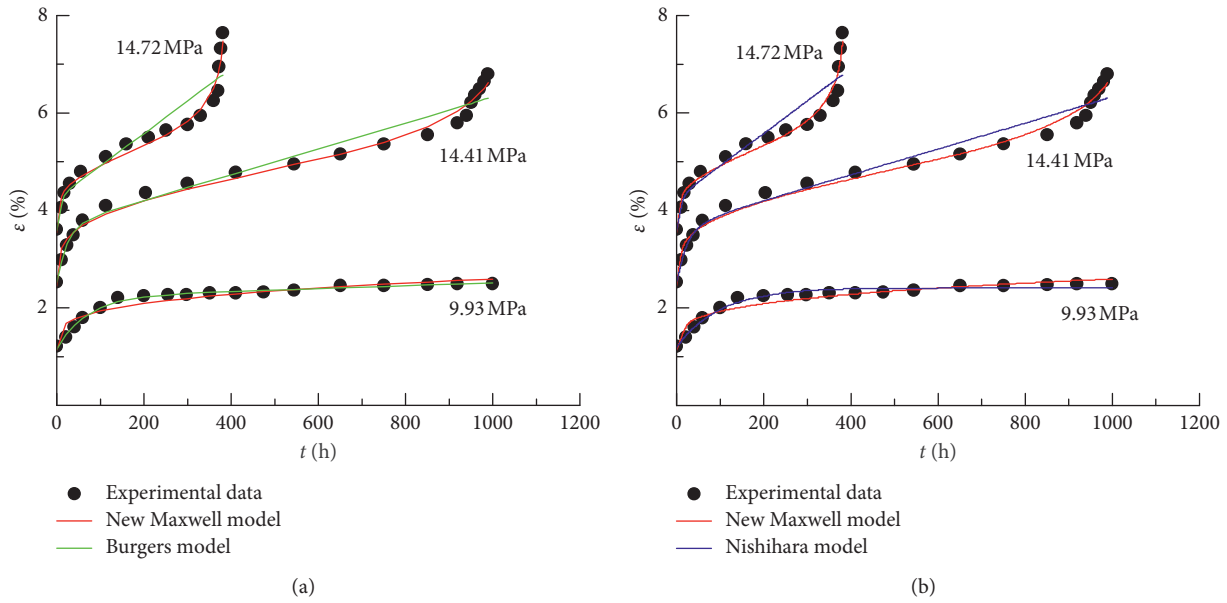

Figure 5: Comparison between theoretical and experimental curves of (a) new Maxwell model and Burgers model and (b) new Maxwell model and Nishihara model.

than the Burgers and Nishihara models when the loading stress is larger than the critical stress, especially for the accelerated creep phase; further, when the loading stress is lower than the critical stress, the new Maxwell creep model can also show good simulation ability, like that of the Burgers model. Overall, the new Maxwell creep model proposed in this work is capable of describing the creep properties of rock, and its structure is very simple, containing only four parameters; therefore, it has high potential for practical applications in rock engineering.

3.3. Sensitivity Studies Using the New Maxwell Creep Model. It is clear that the new Maxwell creep model is advantageous in simulating the accelerated creep stage of rock salt under a 1D stress state. These advantages depend on just a few parameters used in this model, as shown in Equation (9), among which the fractional derivative order β and exponent α are the most important ones. To obtain a better understanding regarding the effects of these parameters, sensitivity analyses were carried out. Substituting $\sigma = 14.41$ MPa, $\sigma_s = 13.5$ MPa, $E = 0.590$ GPa, $\xi = 3.662$ GPa·h$^{\beta}$, $t_F = 1056$ h, and $\alpha = 0.191$ (data from Table 1) into equation (9) and letting the fractional derivative order β change from 0.2 to 0.3 with an interval of 0.02, we obtained a series of curves, as shown in Figure 6; these indicate that the creep strain and creep rate in the steady creep stage mainly depend on the fractional derivative order. Small increments in the fractional derivative order can cause the creep curve to rise in the steady creep stage, thus leading to a greater steady creep strain and higher steady creep strain rate.

By changing exponent α and keeping the other parameters constant, a series of curves were obtained (Figure 7). It is clear that the strain in the accelerated creep stage and creep rate increase with exponent α. Changing α values can realise simulation of the accelerated creep stage with different creep rates.

4. Analysis of New Maxwell Creep Model in 3D Creep State

4.1. Test Conditions and Results. To further explore the ability of the proposed model to simulate the creep behaviour of geotechnical materials under a 3D stress state, the creep results of remolded loess under triaxial conditions were obtained. The loess samples were collected from the L6 loess layer in the new district of Yan'an city; it belongs to the quaternary middle Pleistocene loess, also referred to as the Q_2 loess. The undisturbed loess was ground, dried, and sieved through a 2-mm screen to have a moisture content of 10%; it was kept for 24 h without allowing evaporation to allow the water to be uniformly distributed in the loess. By controlling the compactness levels (k) at 0.84, 0.89, 0.95, and 0.99, the amount of loess required for forming remolded loess under different compactness levels was prepared. The prepared loess was filled into a cylindrical mold to prepare remolded loess specimens and then compressed as per set compression rates using a sample-making machine. The prepared remolded loess specimens were cylinders with diameters and heights of 39.8 and 80 mm, respectively.

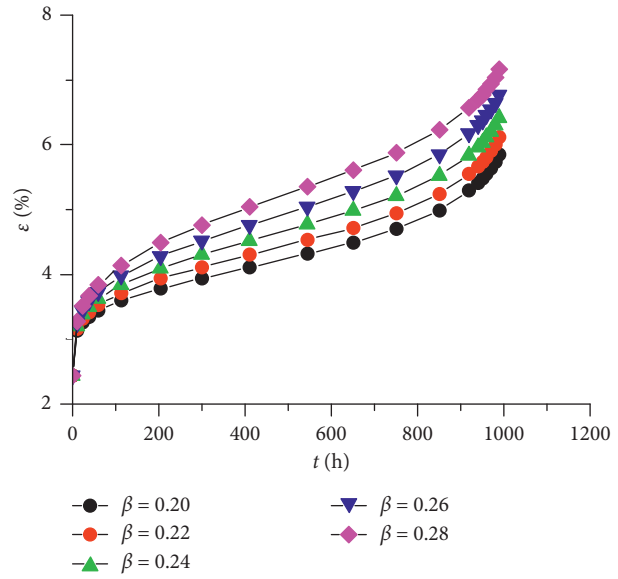

Figure 6: Sensitivity of the creep strain to fractional derivative order β ($\sigma = 14.41$ MPa, $\sigma_s = 13.5$ MPa, $E = 0.590$ GPa, $\xi = 3.662$ GPa·h$^{\beta}$, $t_F = 1056$ h, and $\alpha = 0.191$).

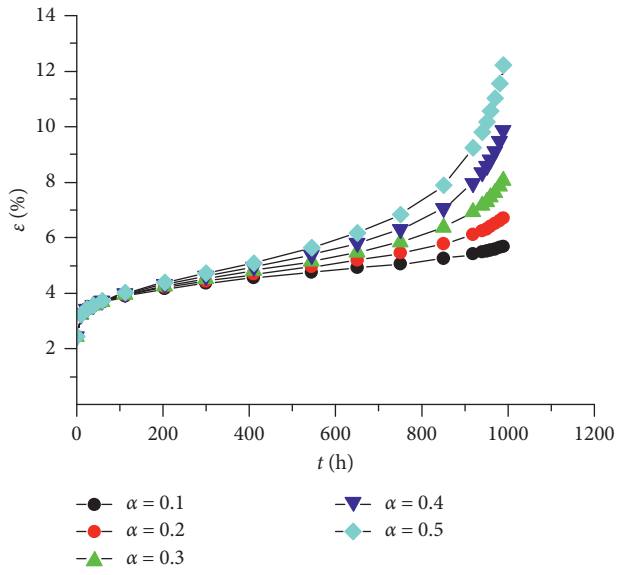

Figure 7: Sensitivity of the creep strain to exponent α ($\sigma = 14.41$ MPa, $\sigma_s = 13.5$ MPa, $E = 0.590$ GPa, $\xi = 3.662$ GPa·h$^{\beta}$, $t_F = 1056$ h, and $\beta = 0.252$).

The SLB-1A stress-strain controlled test machine was used for triaxial creep shear measurements, as shown in Figure 8. This instrument can be stress-loaded through a pneumatic pump, so the set stress can reach a predetermined value in a short time. Before performing the creep tests of remolded loess, the ultimate deviatoric stress values of remolded loess specimens were determined via triaxial consolidated undrained compression tests at a fixed confining pressure of 100 kPa. Under the same confining pressure, the specimens were first consolidated for 24 h; then, indoor creep tests using remolded loess specimens with different compactness levels were conducted under different

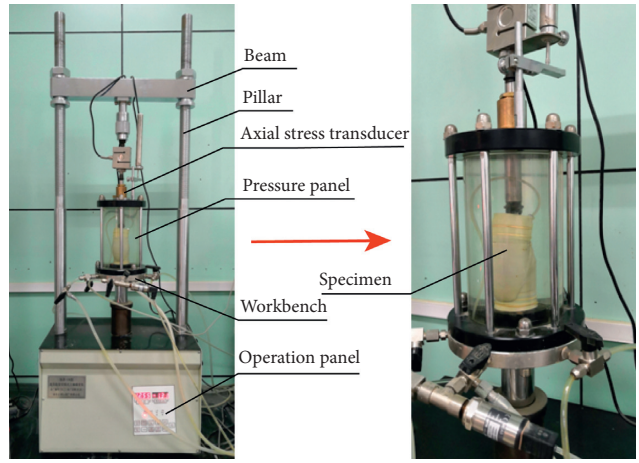

Figure 8: Triaxial creep shear test apparatus: (a) instrument details; (b) creep test state.

axial deviatoric stress levels. The axial deviatoric stress was applied step by step using stress levels of $R = 20$, 40, 60, 80, 90, 95, and 98% (R denotes the ratio of the deviatoric stress to the ultimate stress), and the axial pressure exerted on the specimens during loading was kept constant with a precision of ±5 kPa for 12 h.

A cylindrical specimen was prepared and wrapped on the outside with a rubber film with a tubular mold. Filter paper and permeable stone were placed at both ends of the sample, and the lower end of the sample rubber band was tied to the base and the upper end to the top. Next, the pressure chamber cover was installed and turned on the water switch to fill the pressure chamber with water. At this point, we opened the drain valve and applied the required confining pressure of 100 kPa through stress loading; this pressure was maintained for 24 h to allow the specimen to consolidate. We observed changes in the pore water pressure during consolidation, and we then closed the drain valve and applied axial deviatoric stresses were applied in a stepwise manner at the foregoing levels and recorded axial deformation data using an external strain gauge during creep.

Based on the results of the above creep tests, creep curves at various compactness levels and deviatoric stresses were drawn, as shown in Figure 9. It is evident that axial creep deformations under various compactness levels are roughly similar; the primary, secondary, and tertiary creep stages can be observed under partial deviatoric stress. The specimens at each step during application of the deviatoric stress showed the primary creep stage where the strain rate gradually decreased. After the primary creep stage, the specimens immediately entered the longer secondary creep stage; in this stage, the strain rate tended to be zero under low deviatoric stress; however, under high deviatoric stress, the creep strain increased linearly with time when the strain rate was greater than zero and constant. Next, under a particular high deviatoric stress, the tertiary creep stage developed with time following the secondary creep stage and the axial strain and strain rate significantly increased at this stage.

4.2. Parameter Determination. Considering the creep test results of remolded loess samples with a compactness of 0.95 as an example, we used the 3D creep equation of the new Maxwell model to fit the experimental data. The parameters in equation (15) can also be determined by the Levenberg–Marquardt method, and the results are presented in Table 2. The efficacy of the proposed creep model in fitting the data of remolded loess is shown in Figure 10. To further analyse the ability of the model to describe the accelerated creep stage of remolded loess under a 3D stress state, we selected the creep data corresponding to the last stress loading and compared it to the Burgers and Nishihara models, as shown in Figure 11; the parameters of the Burgers and Nishihara models are given in Table 2.

As observed in Figure 10 and Table 2, the calculated results using the new Maxwell model are in good agreement with the test results obtained under deviatoric stresses of 122, 244, 366, 488, and 550 kPa. The correlation coefficient squares (R^2) of the five curves are 0.974, 0.975, 0.954, 0.978, and 0.996, respectively, indicating that the prediction precision of the new Maxwell creep model is high when simulating the 3D creep properties of remolded loess. According to Figure 11 and Table 2, the accuracies of the Nishihara and Burgers models when fitting the creep test data corresponding to the last stress loading of remolded loess are obviously lower than those of the new Maxwell model. According to the analysis presented above, the new Maxwell creep model is capable of describing the complete creep behaviour of remolded loess, especially the accelerated creep phase, under a 3D stress state.

5. Discussion

To describe the time-dependence of the mechanical properties of geotechnical materials in the entire creep process, a new Maxwell creep model based on fractional derivatives and elastic-plastic elements was developed, and creep constitutive equations were established with explanations. Through simulation capability analysis of the model proposed herein, we found that the new model showed good

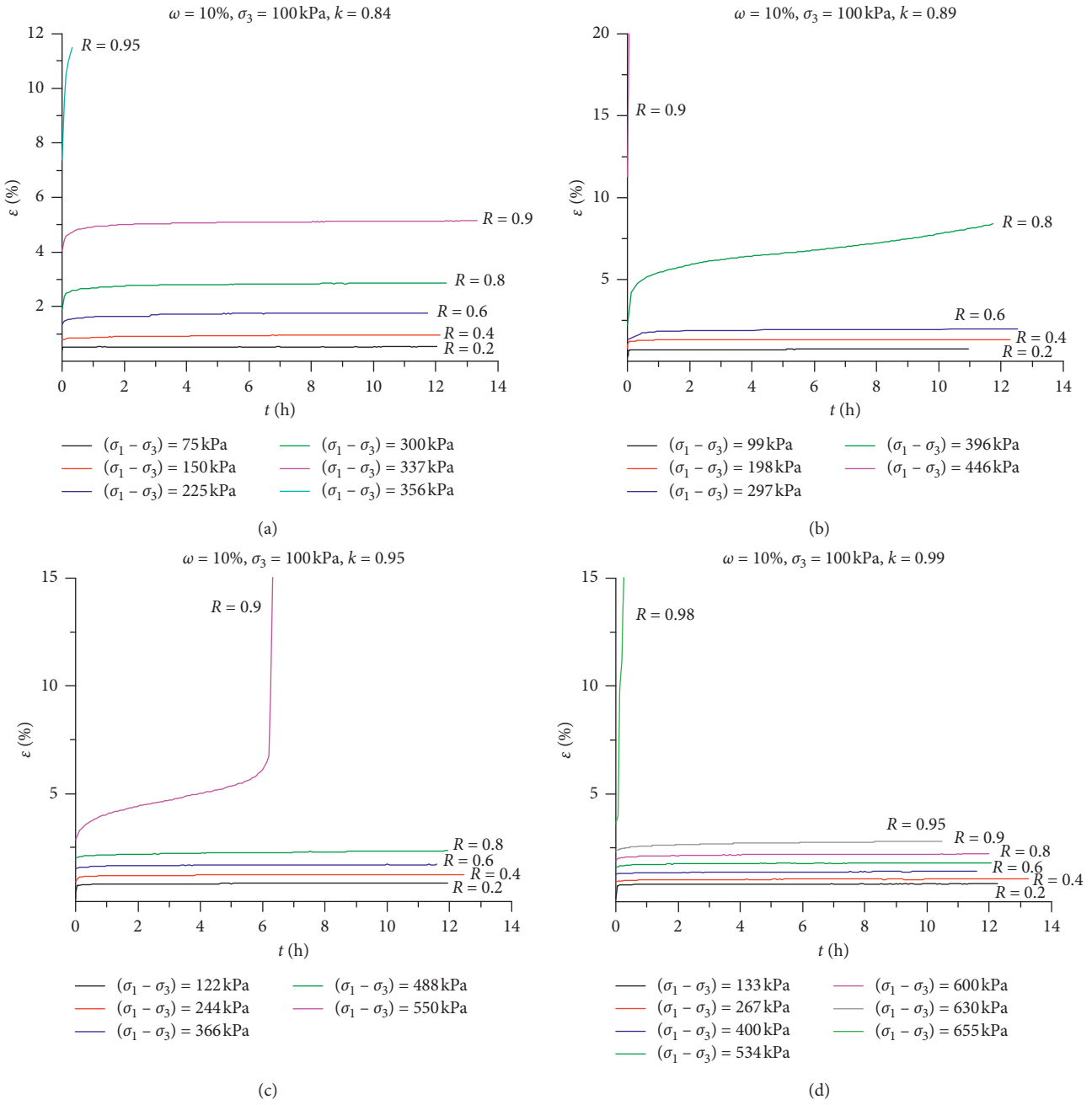

Figure 9: Axial strain versus time at different compactness levels: (a) $k = 0.84$; (b) $k = 0.89$; (c) $k = 0.95$; (d) $k = 0.99$.

Table 2: Parameters determined through fitting the analysis based on creep test results of remolded loess.

	$\sigma_1 - \sigma_3$ (kPa)	G (kPa)	K (kPa)	ξ'(kPa·h$^{\beta}$)	β	α	σ_s (kPa)	t_F (h)	R^2
New Maxwell creep model	122	29856.761	742.362	0.018	0.041				0.974
	244	209.192	91.334	0.003	0.097				0.975
	366	5832.610	42.649	0.001	0.181				0.954
	488	90.682	345.728	0.0008	0.332				0.978
	550	2702.403	33.217	0.005	0.456	0.785	490	6.3	0.998
Burgers model	$\sigma_1 - \sigma_3$ (kPa)	G_0 (kPa)	K (kPa)	G_k (kPa·h)	η_k (kPa·h)	η (kPa·h)			R^2
	550	105.281	48.865	0.235	25516.903	431.671			0.767
Nishihara model	$\sigma_1 - \sigma_3$ (kPa)	G_0 (kPa)	K (kPa)	G_k (kPa·h)	η_k (kPa·h)	η_s (kPa·h)	σ_s (kPa)		R^2
	550	80.301	71.612	0.155	28047.865	47.019	490		0.797

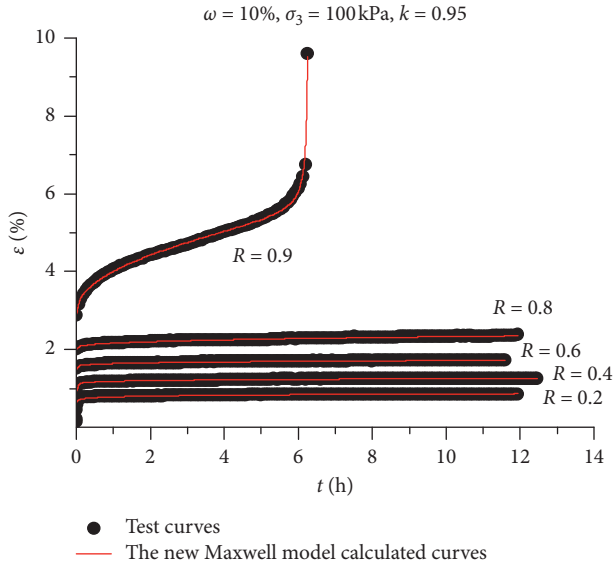

Figure 10: Comparison between theoretical and experimental curves.

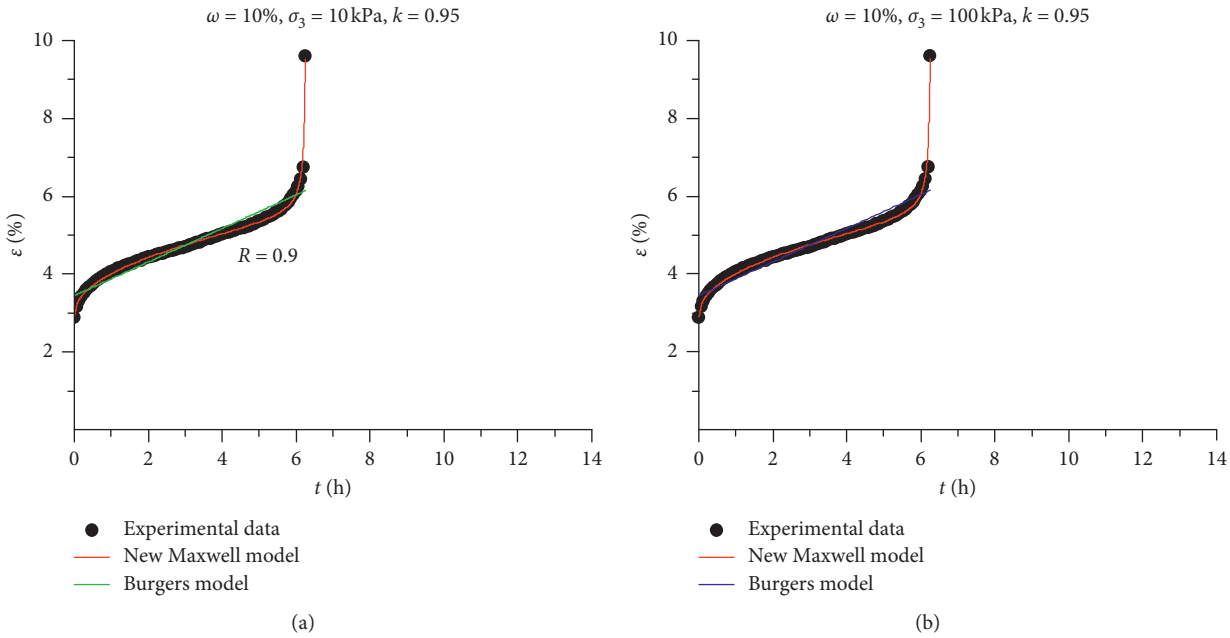

Figure 11: Comparison between theoretical and experimental curves of (a) new Maxwell model and Burgers model and (b) new Maxwell model and Nishihara model.

agreement with the experimental creep data of rock salt and remolded loess, especially for the accelerated creep phase. Further, we can observe from Figure 5 that the new Maxwell creep model has better accuracy in fitting the experimental data of rock salt under a 1D stress state, especially in the case of the intact creep behaviour, compared with the classical Burgers and Nishihara models. The new Maxwell creep model has only two elements and four parameters, thus making it very simple compared to most other creep models; moreover, by changing parameters β and α, the steady creep and accelerated creep stages with different creep rates can be simulated effectively. Similarly, as shown in Figures 10 and 11, compared with the Burgers and Nishihara models, the new Maxwell creep model also has a better effect in describing the creep characteristics of remolded loess under a 3D stress state. In general, our results demonstrate that the new Maxwell creep model can characterise the creep behaviour of geotechnical materials with better accuracy and fewer parameters than extant models. Therefore, this model can be used extensively in the field of geotechnical engineering, and it can help in developing and clarifying creep constitutive models.

6. Conclusions

In this study, we employed fractional and elastic-plastic elements to construct a new Maxwell creep model and derived the corresponding creep functions. The developed model is simple and comprises four parameters and two elements. The fitting results provided by the new Maxwell creep model were also analysed. The results indicate that this model is capable of analysing the creep behaviour of geotechnical materials under different loading conditions. Moreover, it can effectively capture the accelerated creep behaviour of geotechnical materials, which is difficult to observe in most of existing creep models. Additionally, the encouraging results provided by this model can enable other scholars to study the creep models with renewed interest.

Data Availability

The data used to support the findings of this study are included within the article.

Conflicts of Interest

The authors declare that they have no conflicts of interest.

Acknowledgments

The authors gratefully acknowledge the support of the National Natural Science Foundation of China (Grant nos. 41602305, 41790442, 41877266, and 41702298).

References

[1] G. W. Scott Blair, "The role of psychophysics in rheology," *Journal of Colloid Science*, vol. 2, no. 1, pp. 21–32, 1947.

[2] L. Rogers, "Operators and fractional derivatives for viscoelastic constitutive equations," *Journal of Rheology*, vol. 27, no. 4, pp. 351–372, 1983.

[3] R. L. Bagley and P. J. Torvik, "Fractional calculus—a different approach to the analysis of viscoelastically damped structures," *AIAA Journal*, vol. 21, no. 5, pp. 741–748, 1983.

[4] R. L. Bagley and P. J. Torvik, "Fractional calculus in the transient analysis of viscoelastically damped structures," *AIAA Journal*, vol. 23, no. 6, pp. 918–925, 1985.

[5] R. C. Koeller, "Applications of fractional calculus to the theory of viscoelasticity," *Journal of Applied Mechanics*, vol. 51, no. 2, pp. 299–307, 1984.

[6] S. W. J. Welch, R. A. L. Rorrer, and R. G. Duren Jr., "Application of time-based fractional calculus methods to viscoelastic creep and stress relaxation of materials," *Mechanics of Time-Dependent Materials*, vol. 3, no. 3, pp. 279–303, 1999.

[7] H. W. Zhou, C. P. Wang, L. Mishnaevsky Jr., Z. Q. Duan, and J. Y. Ding, "A fractional derivative approach to full creep regions in salt rock," *Mechanics of Time-Dependent Materials*, vol. 17, no. 3, pp. 413–425, 2013.

[8] H. W. Zhou, C. P. Wang, B. B. Han, and Z. Q. Duan, "A creep constitutive model for salt rock based on fractional derivatives," *International Journal of Rock Mechanics and Mining Sciences*, vol. 48, no. 1, pp. 116–121, 2011.

[9] D. S. Yin, Y. Q. Li, H. Wu, and X. M. Duan, "Fractional description of mechanical property evolution of soft soils during creep," *Water Science and Engineering*, vol. 6, no. 4, pp. 446–455, 2013.

[10] J. Kang, F. Zhou, C. Liu, and Y. Liu, "A fractional non-linear creep model for coal considering damage effect and experimental validation," *International Journal of Non-linear Mechanics*, vol. 76, pp. 20–28, 2015.

[11] C. Celauro, C. Fecarotti, A. Pirrotta, and A. C. Collop, "Experimental validation of a fractional model for creep/recovery testing of asphalt mixtures," *Construction and Building Materials*, vol. 36, pp. 458–466, 2012.

[12] J. X. Lai, S. Mao, J. L. Qiu et al., "Investigation progresses and applications of fractional derivative model in geotechnical engineering," *Mathematic Problems in Engineering*, vol. 2016, Article ID 9183296, 15 pages, 2016.

[13] H. Xu and X. Jiang, "Creep constitutive models for viscoelastic materials based on fractional derivatives," *Computers & Mathematics with Applications*, vol. 73, no. 6, pp. 1377–1384, 2017.

[14] Z. Xu and W. Chen, "A fractional-order model on new experiments of linear viscoelastic creep of Hami Melon," *Computers & Mathematics with Applications*, vol. 66, no. 5, pp. 677–681, 2013.

[15] Y. Liu, J. Shan, and N. Qi, "Creep modeling and identification for piezoelectric actuators based on fractional-order system," *Mechatronics*, vol. 23, no. 7, pp. 840–847, 2013.

[16] H. Tang, Z. Duan, D. Wang, and Q. Dang, "Experimental investigation of creep behavior of loess under different moisture contents," *Bulletin of Engineering Geology and the Environment*, vol. 79, no. 1, pp. 411–422, 2020.

[17] F. Wu, J. F. Liu, and J. Wang, "An improved maxwell creep model for rock based on variable-order fractional derivatives," *Environment Earth Science*, vol. 73, no. 11, pp. 6955–6971, 2015.

[18] C. Mazzotti and M. Savoia, "Nonlinear creep damage model for concrete under uniaxial compression," *Journal of Engineering Mechanics*, vol. 129, no. 9, pp. 1065–1075, 2003.

[19] E. Verstrynge, L. Schueremans, and D. Van Gemert, "Time-dependent mechanical behavior of lime-mortar masonry," *Materials and Structures*, vol. 44, no. 1, pp. 29–42, 2011.

[20] L.-J. Ma, X.-Y. Liu, Q. Fang et al., "A new elasto-viscoplastic damage model combined with the generalized hoek-brown failure criterion for bedded rock salt and its application," *Rock Mechanics and Rock Engineering*, vol. 46, no. 1, pp. 53–66, 2013.

[21] W. G. Cao, J. Z. Yuan, J. Y. Wang, and Y. C. Zhai, "A damage simulation technique of the full rock creep process considering accelerated creep," *Journal of Hunan University (Natural Science)*, vol. 40, no. 2, pp. 15–20, 2013.

[22] M. Kachanov, "Effective elastic properties of cracked solids: critical review of some basic concepts," *Applied Mechanics Reviews*, vol. 45, no. 8, pp. 304–335, 1992.

[23] T. T. Cai, Z. C. Feng, and Y. L. Jiang, "An improved hardening-damage creep model of lean coal: a theoretical and experimental study," *Arabian Journal of Geoscience*, vol. 11, no. 20, pp. 1–12, 2018.

[24] R. Wang, Y. Jiang, C. Yang, F. Huang, and Y. Wang, "A nonlinear creep damage model of layered rock under unloading condition," *Mathematical Problems in Engineering*, vol. 2018, Article ID 8294390, 8 pages, 2018.

[25] D. Li, J. Chen, and Y. Zhou, "A study of coupled creep damaged constitutive model of artificial frozen soil," *Advances in Materials Science and Engineering*, vol. 2018, Article ID 7458696, 9 pages, 2018.

[26] H. Z. Liu, H. Q. Xie, J. D. He, M. L. Xiao, and L. Zhuo, "Nonlinear creep damage constitutive model for soft rocks,"

Mechanics of Time-Dependent Materials, vol. 21, no. 1, pp. 73–96, 2017.

[27] I. Colombaro, A. Giusti, and F. Mainardi, "A one parameter class of fractional Maxwell-like models," in *Proceedings of the American Institute of Physics Conference Series*, vol. 1836, no. 1, pp. 1–6, Bydgoszcz, Poland, June 2017.

[28] X. Ding, G. Q. Zhang, B. Zhao, and Y. Wang, "Unexpected viscoelastic deformation of tight sandstone: insights and predictions from the fractional maxwell model," *Scientific Reports*, vol. 7, no. 1, pp. 1–11, 2017.

[29] A. Hernández-Jiménez, J. Hernández-Santiago, A. Macias-García, and J. Sánchez-González, "Relaxation modulus in PMMA and PTFE fitting by fractional maxwell model," *Polymer Testing*, vol. 21, no. 3, pp. 325–331, 2002.

[30] H. Schiessel, R. Metzler, A. Blumen, and T. F. Nonnenmacher, "Generalized viscoelastic models: their fractional equations with solutions," *Journal of Physics A: Mathematical and General*, vol. 28, no. 23, pp. 6567–6584, 1995.

[31] C. Friedrich, "Relaxation and retardation functions of the maxwell model with fractional derivatives," *Rheologica Acta*, vol. 30, no. 2, pp. 151–158, 1991.

[32] W. C. Tan, W. X. Pan, and M. Y. Xu, "A note on unsteady flows of a viscoelastic fluid with the fractional maxwell model between two parallel plates," *International Journal of Non-linear Mechanics*, vol. 38, no. 5, pp. 645–650, 2003.

[33] I. Podlubny, "The laplace transform method for linear differential equations of the fractional order," *Fractional Differential Equations*, Academic Press, San Diego, CA, USA, 1999.

[34] X. D. Qiu, Y. D. Jiang, Z. L. Yan, and Q. C. Zhuang, "Creep damage failure of rock salt," *Journal of Chongqing University*, vol. 26, no. 5, pp. 106–109, 2003.